

Analysis Of Thresholds In Rule-Based Antilock Braking Control Algorithms^{*}

Akhil Challa, Karthik Ramakrushnan, Shankar C. Subramanian^{*}
Gunasekaran Vivekanandan, Sriram Sivaram^{**}

^{*} Indian Institute of Technology Madras, Chennai, TN, 600036, INDIA
(e-mail: shankarram@iitm.ac.in)

^{**} Madras Engineering Industries Pvt. Ltd. Chennai, TN, 603209, INDIA

Abstract: An Antilock Braking System (ABS) is an Active Vehicle Safety System (AVSS) employed to prevent wheel lock in road vehicles. Wheel lock is undesirable as it may lead to loss of vehicle steerability and directional stability. These become critical in Heavy Commercial Road Vehicles (HCRVs) as unintentional yaw motion resulting from directional instability may also lead to vehicle roll-over. ABS algorithms are broadly classified as Model-Based Algorithms (MBAs) and Rule-Based Algorithms (RBAs). MBAs are typically physics based and employ vehicle dynamic models. RBAs, which are currently predominantly used in vehicles, are threshold based. RBAs require measurement of wheel speed that is readily available, while MBAs require real time information on vehicle parameters and tire models. Most commercially available RBAs are proprietary and the details are not revealed. This has motivated the present study, and the physical significance of the wheel slip and wheel acceleration thresholds used in RBAs are clearly identified, backed by experiments from a Hardware-in-Loop (HiL) pneumatic brake setup along with IPG TruckMaker[®], a software for vehicle dynamic simulation. This study is an important first step in developing an advanced RBA for HCRVs.

© 2020, IFAC (International Federation of Automatic Control) Hosting by Elsevier Ltd. All rights reserved.

Keywords: Rule Based Algorithm, Antilock Braking System, Wheel acceleration, Wheel slip, Thresholds.

1. INTRODUCTION

Increasing number of road vehicles and the advancements in their design for operating at higher speeds make it imperative to equip drivers with Active Vehicle Safety Systems (AVSSs). Road vehicle fatalities are one of the chief concerns all over the world. The World Health Organization (WHO) reported a staggering number of 1.35 million traffic fatalities in 2016 [World Health Organization (2018)]. The Ministry of Road Transport and Highways (MoRTH), Government of India, reported that 4,64,910 accidents occurred in 2017 [Ministry of Road Transport and Highways (2018)]. Although Heavy Commercial Road Vehicles (HCRVs) constitute only 5.4% of the vehicle population in India, they account for nearly 32.6% of fatalities. WHO has recently added Anti-Lock Braking System (ABS) requirement as a priority standard. MoRTH has also mandated ABS in HCRVs for the M3 and N3 category of vehicles in the year 2016. These statistics and adapting standards motivate the need for developing an ABS algorithm for HCRVs, to avoid wheel lock and reduce braking distances, hence minimizing road fatalities. To do so, the understanding of existing Rule-Based Algorithm (RBA) techniques for ABS is essential. This work pro-

poses a systematic methodology for examining the use of thresholds that are used in such algorithms.

ABS falls under the category of Wheel Slip Regulation (WSR) algorithms where wheel slip is the controlled variable. When the wheel stops rotating while the vehicle is still in motion, it is said to lock. Wheel slip ratio (λ) captures this effect and is defined as

$$\lambda(t) = \frac{v_x(t) - r\omega(t)}{v_x(t)}, \quad (1)$$

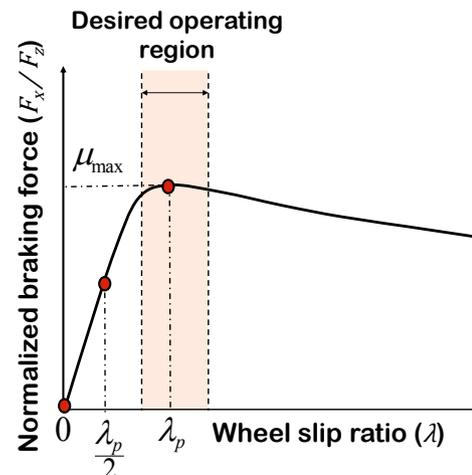


Fig. 1. Normalized braking force - wheel slip curve

^{*} Funding provided by the Ministry of Skill Development and Entrepreneurship, Government of India, through the grant EDD/14-15/023/MOLE/NILE, and Madras Engineering Industries Private Limited, Chennai, India, through the grant RB1617EDD004MADACSSH.

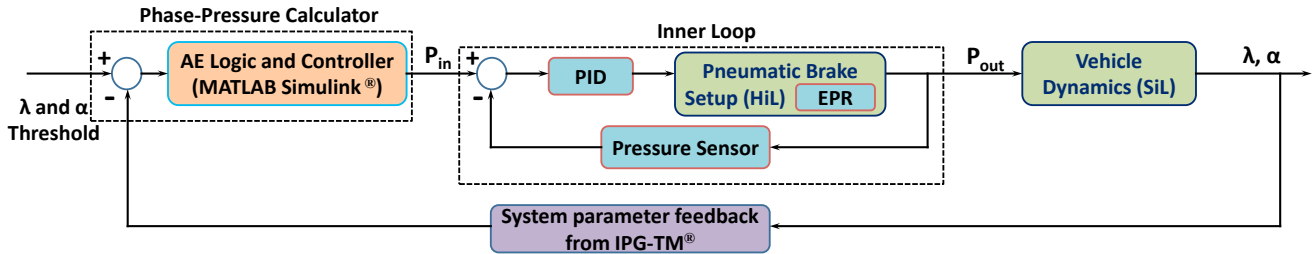


Fig. 2. Block level diagram of the control loops involved in threshold analysis

where v_x is the vehicle longitudinal speed at time t , ω is the wheel angular speed and r is the tire radius. Wheel slip ratio has a non-linear relationship with the longitudinal traction force available at the tire-road interface as depicted in Fig. 1. ABS algorithms desire to maintain slip in the region marked in Fig. 1, in order to exploit maximum tire-road traction forces and avoid wheel lock. Here, μ_{max} is the maximum tire-road friction coefficient and λ_p is the wheel slip at which the former occurs.

Figure 2 presents the block level diagram of the control loops involved in this work. The inner loop consists of the Electro Pneumatic Regulator (EPR) and the pressure sensor. A PID controller regulates the performance of EPR valve. In outer loop, the plant is constituted of two parts. The pneumatic brake subsystem (of the entire vehicle) alone is a Hardware-in-Loop (HiL) setup, and rest of the vehicle dynamics is modelled in IPG-TruckMaker[®] (IPG-TM) and is Software-in-Loop (SiL) simulated. Two important variables (wheel slip ratio (λ) and wheel acceleration (α)) are fed back from IPG-TM to the comparator of the outer loop. The inputs to the comparator are the λ and α thresholds from the user. Then, the Apply Exhaust (AE) logic programmed in MATLAB/Simulink[®] decides for the implementation of an Apply (1) or an Exhaust (0) phase. All the blocks are elaborated in the forthcoming sections.

Commercial ABS systems employ RBAs consisting of fixed thresholds for different parameters, and a set of rules that dictate the control action. ABS logic of Bosch (Reif (2015)), which is widely used in hydraulic brake systems of passenger cars proposes an 8-phase logic that switches control action depending upon the values of λ and α . The control actions used are pumping (increasing brake pressure), dumping (releasing brake pressure), holding (keeping the brake pressure constant at its current value) and pump-hold (increasing brake pressure in steps). The algorithm utilizes one wheel slip threshold (λ_1) and three wheel acceleration thresholds ($-a$, $+a$, and $+A$). WABCO and Knorr-Bremse are two other popular ABS solutions employed in HCRVs with pneumatic brake systems. For example, WABCO (2006) ABS algorithm employs two wheel slip thresholds (λ_1 and λ_2) and two wheel acceleration thresholds ($-b$ and $+b$). The control actions of this algorithm also include pumping, dumping, holding and pump-hold.

The key takeaways from these algorithms were:

- Commercial Rule-based ABS algorithms utilize both wheel slip and wheel acceleration thresholds.

- The motivation behind the choice of these variables and their thresholds are proprietary and not revealed.

This motivated the need for analyzing the aforementioned variables, and an investigation into their thresholds.

2. LITERATURE SURVEY

Literature survey was carried out to understand existing knowledge on the implementation of RBAs. Kuo and Yeh (1992) designed a 4-phase control scheme for an ABS application. The authors performed computer simulations to evaluate their algorithm considering a piece-wise linear tire model, and the thresholds used for the control parameters were computed using vehicle dynamic equations. Tao and Wang (1999) designed a 4-phase control logic for an ABS application with dynamic thresholds, also determined using approximated vehicle dynamics equations. Ait-Hammouda and Pasillas-Lépine (2004) and Pasillas-Lépine (2006) considered a class of 5-phase ABS control algorithms and characterized their behaviour with limit cycle and Poincare map analysis. Further, they proposed an improved 11-phase strategy towards improving robustness over different road surfaces, using Simulink[®] simulations. Gerard et al. (2010) and Gerard et al. (2012) proposed improvements to existing 5-phase ABS algorithms and evaluated the improved algorithm using Tire-in-the-loop testing. Penny et al. (2016) modified the Bosch 8-phase algorithm to also include a dump-hold action, and developed an embedded ABS controller to test it on a vehicle. Wan and Xiong (2016) designed an optimal self adjusting threshold control for ABS, where the threshold values change according to the speed and road conditions. A 2-wheel vehicle dynamic model, along with Magic Formula tire model for longitudinal dynamics were used, and MATLAB[®] simulations were performed to identify the range of threshold values.

Existing literature was found to focus more on implementation and analysis of RBAs for passenger cars. However, no such analysis regarding the physics behind the selection of thresholds, or investigation into their values were done for both passenger cars as well as HCRVs. Further, most of the papers utilized software simulations for evaluating their algorithms. These gaps in literature were addressed in this work.

3. EXPERIMENTAL SETUP

The HiL experimental facility, shown in Fig. 3, consists of front and rear axles of a four wheeled 16 tonne HCRV attached to custom made fixtures. Front axle incorporates

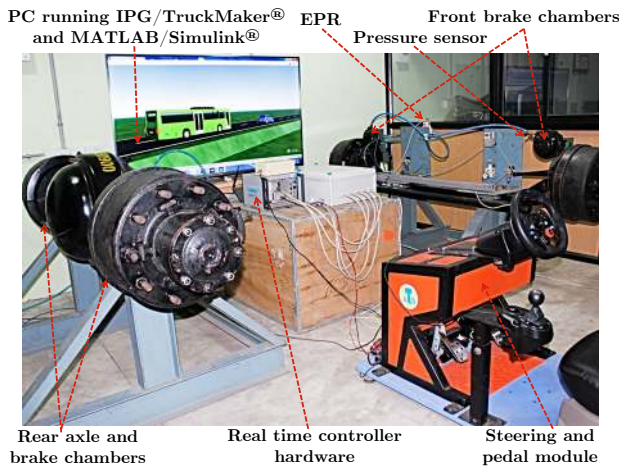


Fig. 3. HiL setup used for experimentation

two Type-20 brake chambers whereas the rear has two Type-20/24 chambers. The foundation brakes used are S-cam actuated drum brakes. Each brake chamber has a pressure sensor and an EPR (used for metering out compressed air). The pressure sensors used have a range of 100-1100 kPa and the EPR input is in the range of 0-10 V. IPG TruckMaker[®] was the vehicle dynamic simulation software used that is co-simulated with MATLAB/Simulink[®] to evaluate WSR algorithms. The interface between the hardware braking setup and the software is through the real time rapid prototyping hardware - IPG XPACK4[®].

4. EXPERIMENTATION METHODOLOGY

A systematic procedure has been adopted for understanding the importance of individual thresholds (wheel slip and wheel acceleration). These two parameters were selected because they characterize wheel and vehicle dynamics during braking. Through the tests that are presented in Table 1, the system's response to wheel slip and wheel acceleration thresholds, both individually and in a combined manner, were recorded and would be detailed. HiL tests were performed for an unladen 16 tonne vehicle (4700 kg) running on a road with peak traction coefficient (μ_{max}) of 0.8. The brakes were applied at an initial braking speed of 80 km/h. Braking starts at 8.8 s for these maneuvers. Figure 4 shows the overall block diagram of the AE logic used. The AE

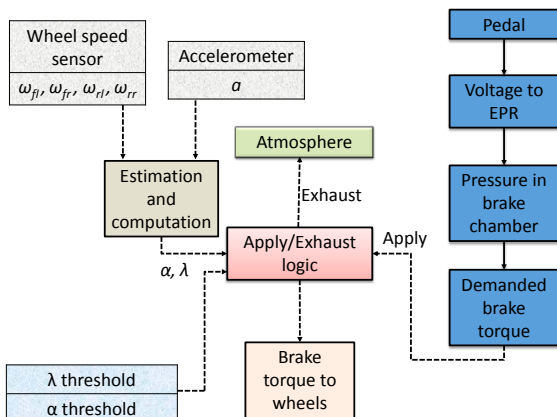


Fig. 4. Block diagram of Apply-Exhaust Logic

logic has input from the driver's brake pedal (pump phase) and the exhaust of compressed air (dump phase) is let to atmosphere. It also takes in the values of thresholds along with vehicle acceleration and wheel angular speeds from respective sensors. Table 1 gives the various tests that were performed in a sequence to gain understanding of the thresholds, and their magnitudes to be considered. Forthcoming sections explain the progression and selection of the test cases. They also deal with each case that was experimented, and presents the understandings obtained.

5. INVESTIGATION OF THRESHOLDS IN RBAs

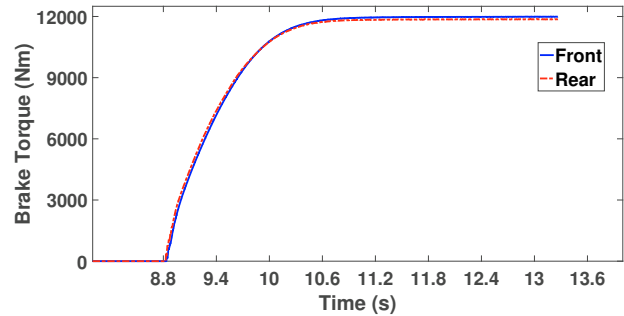


Fig. 5. Open loop panic brake torque applied

The results and observations from HiL experiments are presented in this section. Table 2 details in summary, the performance metrics of each of the test cases performed, shown in Table 1, including the braking distance. Also, the band in which wheel slip and wheel acceleration were regulated are identified in the comments column.

5.1 Open loop tests

This section deals with test cases 1 and 2. Open loop tests without the AE logic for brake torque control, were performed to serve as a benchmark in terms of braking distance comparison. The brake torques applied on the front and rear wheels are depicted in Fig. 5. The braking distance was observed to be 49.89 m for case 1. It was observed that both the front and rear wheels locked in this test. The plots of slip and angular acceleration with respect to time for the front wheels are given in Fig. 6. A similar response was observed for the rear wheels as well.

From the slip response, 3 regions were identified. The first region extends from 0 % slip till 10 % slip. The second

Table 1. HiL Tests with AE logic

Case	Feature
1	Open loop
2	Open loop along with inner loop brake control
Inner loop brake controller is included in all further tests	
3	α_l (rad/s ²) wheel acceleration threshold
4	$\alpha_l/2$ (rad/s ²) wheel acceleration threshold
5	slip threshold lesser than $\lambda_p/2$
6	$\lambda_p/2$ slip threshold
7	slip threshold greater than $\lambda_p/2$
8	slip threshold closer to λ_p
Following tests also include slip threshold used in case 8	
9	α_l (rad/s ²) wheel acceleration threshold
10	α_l and α_h (rad/s ²) wheel acceleration threshold

Table 2. Table of Observations

Test Case	Braking Distance (m)	Comments on λ and α regulation
1	49.89	Benchmark for braking distance comparison
2	49.67	Benchmark for braking distance comparison
3	48.27	WL* α spikes to a value greater than α_l and then settles at zero
4	42.07	Slightly better regulation at the start, but finally WL* α spikes to a value greater than α_l and then settles at zero
5	41.42	λ : 9 - 10 % α : - 40 to 40 rad/s^2
6	39.99	λ : 10 %, ML** α : - 50 to 50 rad/s^2
7	39.85	λ : 10 to 15 %, One instance of lock at higher speed α : - 100 to 100 rad/s^2
8	40.94	λ : 10 - 15 %, ML** α : -150 to 150 rad/s^2
9	39.6	λ : 10 - 18 %, ML** α : - 40 to 50 rad/s^2
10	39.25	λ : 10 - 18 %, ML** α : - 40 to 50 rad/s^2

* Eventual wheel lock for rest of the maneuver

** Momentary locks at low speeds

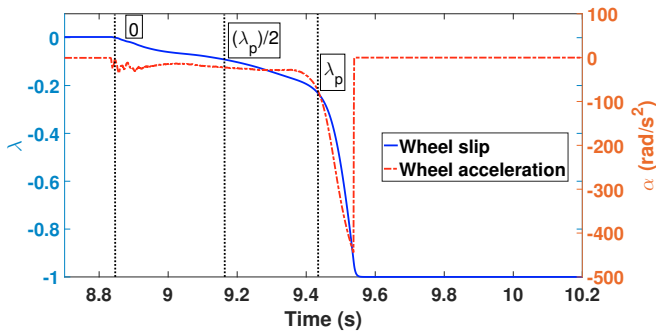


Fig. 6. Open loop response for front wheel

region is from 10 % to 20 %, and the third ranges from 20 % to 100 %, which is the unstable region where rapid wheel lock occurs. The first and the second regions were observed to be in the stable region of the normalized braking force - wheel slip ($\mu - \lambda$ curve shown in Fig. 1). The region to the left and right of λ_p are the stable and unstable regions respectively. The value of λ_p is around 20 % for a dry surface of μ_{max} of 0.8 [Wong (2001)] and the first region is seen to last till half the value of λ_p . The same behaviour was observed for tests performed over different tire-road traction coefficients. Thus, the value of $\lambda_p/2$ seems to be significant and might play an important role in deciding the intervention of the algorithm. Hence, the following tests have used this threshold for experimentation on WSR. One other important parameter is the value of lower acceleration threshold, α_l (-40 rad/s^2), with respect to wheel acceleration. From Fig. 6, it can be observed that after the value of α_l there is a steep decline in wheel acceleration values towards wheel lock. Hence, this parameter was also considered for experimentation on WSR.

Test case 2, in addition to the case 1, has an inner loop PID brake controller included to improve the dynamic response of EPR. The braking distance was observed to be 49.67 m, a marginal improvement over case 1, owing to the quickness in the response of the EPR. The wheels lock in this test too. Similar dynamics were observed in this case also, similar to case 1 with the exception of quicker rise time in their responses. Following test cases 1 and 2, it was decided to investigate the significance of the slip value of $\lambda_p/2$ and α_l . Tests employing slip thresholds just above and below $\lambda_p/2$ and the involvement of the wheel acceleration threshold in the AE logic were tried out.

5.2 Wheel acceleration threshold alone

Figure 7 depict the wheel slip response and the brake torques that were modulated according to the AE logic employed for front wheels.

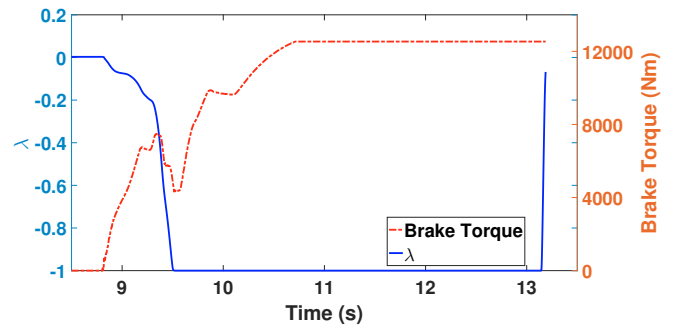


Fig. 7. Slip regulation for front wheels where $\alpha_l = -40 rad/s^2$

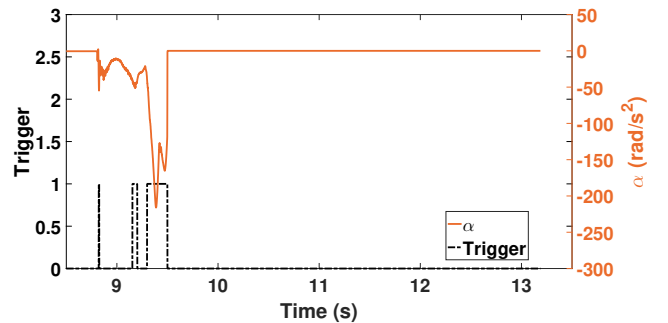


Fig. 8. Wheel acceleration response for front wheels where $\alpha_l = -40 rad/s^2$

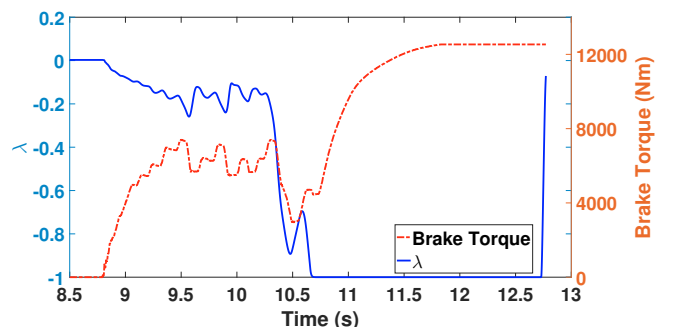


Fig. 9. Slip regulation for front wheels where $\alpha_l = -20 rad/s^2$

Figure 8 shows the corresponding response of wheel acceleration and the trigger plots between the apply (1) and exhaust (0) phase. This is the first test case where control is attempted to prevent lock. The controller here works on AE logic where maximum brake torque is applied when wheel acceleration is lesser in magnitude than the threshold value of -40 rad/s^2 and the brakes are released/exhausted when wheel acceleration exceeds the same. This value was selected from the observations of case 1 and 2. Once the wheel acceleration values cross -40 rad/s^2 wheels very quickly go to lock and it is difficult to bring them back from lock. In test case 4 a stricter threshold of -20 rad/s^2 was introduced to check whether it would help in improving ABS performance. Slip regulation was slightly better than the previous case as shown in Fig. 9, but could not prevent wheel lock. It is concluded from case 3 and 4 that, wheel acceleration by itself is not sufficient for RBAs.

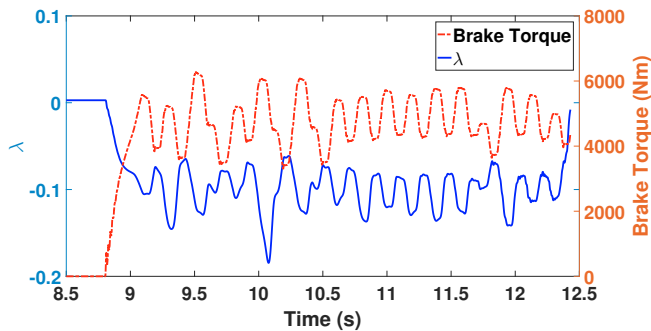


Fig. 10. Slip regulation for front wheels where $\lambda_{th} = 9 \%$

5.3 Wheel slip threshold alone

This section deals with cases 5-8. This is the first test case where slip control using wheel slip thresholds is attempted. The significance of region 1 identified in case 1, was experimented. With reference to test case 5 (employing a slip threshold of 9%), maximum brake torque is demanded and applied when slip is below 9% and the brakes are released/exhausted when slip exceeds 9% . The slip was maintained at around 9 to 10% with occasional fluctuations to about 18% , as shown in Fig. 10. The braking distance is observed to be 41.42 m , a reduction of almost 8 m from the previous test cases (without any slip control). This phenomenon is because of the fact that when the wheels lock (case 1 and 2), the braking force available at the tire-road interface reduces very drastically and hence higher braking distances. Whereas if the system is controlled and operated at a wheel slip value of 9% , although the utilization of braking force is sub-optimal, the values of braking force are higher than in a case where wheels lock. Since the wheel slips were maintained below λ_p , naturally it was observed that the wheel accelerations were maintained in the band of $\pm 40 \text{ rad/s}^2$ (stable α values). The same is depicted in Fig. 11. One another parameter, identified in this test, is the upper wheel acceleration threshold, α_h ($+40 \text{ rad/s}^2$).

Moving further to case 6 (slip threshold of 10%), there is reduction in braking distance (seen in Table 2) because of operating at higher slip thresholds. The wheel slip and wheel acceleration response are shown in Figs. 12 and 13.

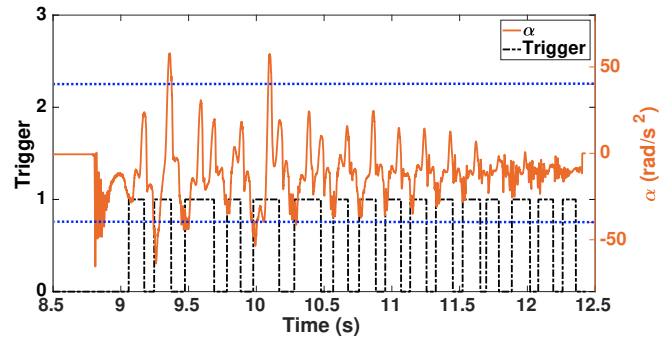


Fig. 11. Wheel acceleration response for front wheels where $\lambda_{th} = 9 \%$

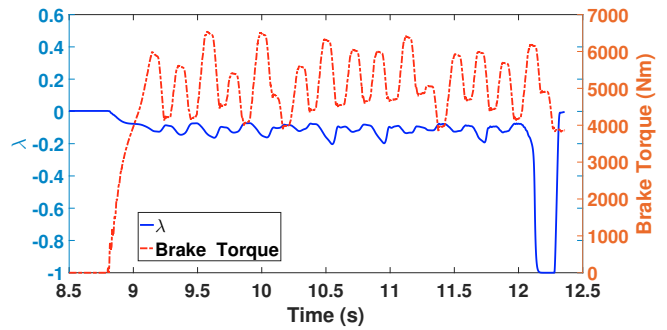


Fig. 12. Slip regulation for front wheels where $\lambda_{th} = 10 \%$

The same is observed in case 7 (slip threshold of 11%), but moving to 12% slip threshold in case 8, resulted in increased the stopping distance. This is due to operating at values greater than $\lambda_p/2$, where slip regulation and wheel lock prevention is not possible with slip threshold alone. Figures 14 and 15 show the system response for case 8. It is clear that at instances of wheel lock, wheel accelerations have exceeded -40 rad/s^2 and were not controlled. Hence, it is concluded that slip threshold alone is not sufficient for preventing wheel lock.

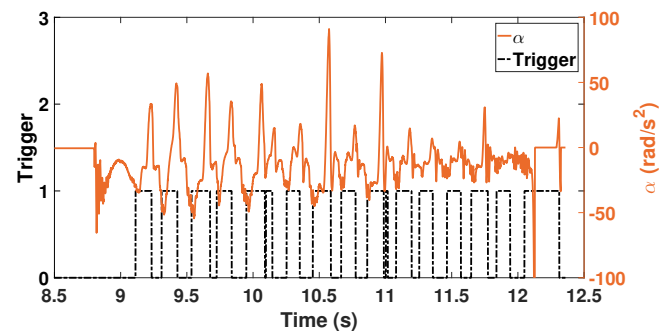


Fig. 13. Wheel acceleration response for front wheels where $\lambda_{th} = 10 \%$

5.4 Wheel slip along with wheel acceleration thresholds

This section deals with cases 9 and 10 and are follow up cases from case 8. Here AE logic was applied with an additional condition of an OR logic between the slip and wheel acceleration thresholds. When either one of them exceeds or is within the set thresholds, a corresponding apply or exhaust logic is implemented. Improvement in

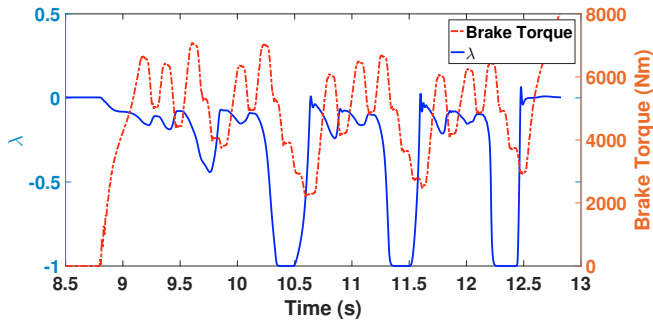


Fig. 14. Slip regulation for front wheels where $\lambda_{th} = 12\%$

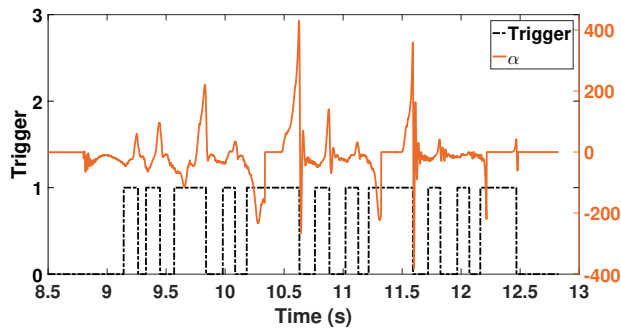


Fig. 15. Wheel acceleration response for front wheels where $\lambda_{th} = 12\%$

the stopping distances (as in Table 2) illustrates the importance of utilizing the wheel acceleration thresholds along with wheel slip thresholds to operate at higher slips greater than $\lambda_p/2$. Better slip regulation and prevention of wheel lock is observed as shown in Fig. 16 for test case 10. However, wheel lock is observed at lower speeds. This is because, in this work a basic on-off type AE logic was used in the outer loop, to analyse the thresholds. Hence, it was not possible to completely avoid wheel lock closer to crawling speeds ($V < 2.5$ km/h) [Reif (2015)]. A properly designed ABS logic that can utilize the understandings obtained in this study can possibly avoid complete wheel lock and simultaneously improve the braking performance, which would be a part of future work.

6. CONCLUSION

This work proposed and demonstrated a framework for experimenting and understanding the different thresholds required for the implementation of a rule-based ABS

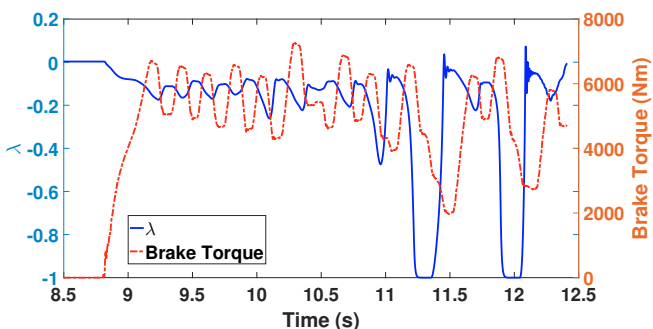


Fig. 16. Slip regulation for front wheels where $\lambda_{th}=12\%$, $\alpha_l=-40$ rad/s² and $\alpha_h=+40$ rad/s²

algorithm (RBA), and their magnitudes. It was observed that neither of wheel slip nor wheel acceleration threshold alone are sufficient to regulate wheel slip beyond $\lambda_p/2$. The importance of wheel slip along with the wheel acceleration threshold, employed in a combined manner to prevent wheel lock, has been presented. Also, the scientific basis behind the selection of threshold values has been related to and explained with the help of normalized traction - wheel slip curve. From the understandings obtained, development of an advanced RBA would be taken up as future work.

REFERENCES

- Ait-Hammouda, I. and Pasillas-Lépine, W. (2004). On a class of eleven-phase anti-lock brake algorithms robust with respect to discontinuous transitions of road characteristics. *IFAC Proceedings Volumes*, 37(21), 551–556.
- Gerard, M., Pasillas-Lépine, W., De Vries, E., and Verhaegen, M. (2010). Adaptation of hybrid five-phase abs algorithms for experimental validation. *IFAC Proceedings Volumes*, 43(7), 13–18.
- Gerard, M., Pasillas-Lépine, W., de Vries, E., and Verhaegen, M. (2012). Improvements to a five-phase abs algorithm for experimental validation. *Vehicle System Dynamics*, 50(10), 1585–1611.
- Kuo, C. and Yeh, E. (1992). A four-phase control scheme of an anti-skid brake system for all road conditions. *Proceedings of the Institution of Mechanical Engineers, Part D: Journal of Automobile Engineering*, 206(4), 275–283.
- Ministry of Road Transport and Highways (2018). Road accidents in India 2017.
- Pasillas-Lépine, W. (2006). Hybrid modeling and limit cycle analysis for a class of five-phase anti-lock brake algorithms. *Vehicle System Dynamics*, 44(2), 173–188.
- Penny, W.C.W. et al. (2016). *Anti-lock braking system performance on rough terrain*. Ph.D. thesis, University of Pretoria.
- Reif, K. (ed.) (2015). *Automotive Mechatronics: Automotive Networking, Driving Stability Systems, Electronics*. Robert Bosch GmbH.
- Tao, J. and Wang, B. (1999). Study of the dynamic threshold and control logic on anti-lock brake system (abs). In *Proceedings of the IEEE International Vehicle Electronics Conference (IVEC'99)(Cat. No. 99EX257)*, 82–85. IEEE.
- WABCO (2006). ABS/ASR D- cab version: Anti-lock braking system for commercial vehicles. Technical report.
- Wan, N. and Xiong, J. (2016). Abs self-adjustment threshold control based on matlab. In *International Conference on Green Intelligent Transportation System and Safety*, 349–355. Springer.
- Wong, J.Y. (2001). *Theory of ground vehicles*. John Wiley & Sons, Inc., New York.
- World Health Organization (2018). Global status report on road safety 2018. Technical report.